

Visual Display Aid for Orbital Maneuvering: Design Considerations

Arthur J. Grunwald*

*Technion—Israel Institute of Technology, Haifa 32000, Israel
and*

Stephen R. Ellis†

NASA Ames Research Center, Moffett Field, California 94035

This paper describes the development of an interactive proximity operations planning system that allows on-site planning of fuel-efficient multiburn maneuvers in a potential multispacecraft environment. Although this display system most directly assists planning by providing visual feedback to aid visualization of the trajectories and constraints, its most significant features include 1) the use of an "inverse dynamics" algorithm that removes control nonlinearities facing the operator, and 2) a trajectory planning technique that separates, through a "geometric spreadsheet," the normally coupled complex problems of planning orbital maneuvers and allows solution by an iterative sequence of simple independent actions. The visual feedback of trajectory shapes and operational constraints, provided by user-transparent and continuously active background computations, allows the operator to make fast, iterative design changes that rapidly converge to fuel-efficient solutions. The planning tool provides an example of operator-assisted optimization of nonlinear cost functions.

Introduction

Orbital Environment

THE proximate orbital environment of future spacecraft in low Earth orbit (LEO) may include a variety of spacecraft co-orbiting in close vicinity. Most of these spacecraft will be "parked" in a stable location with respect to each other, i.e., they will be on the same circular orbit. However, some missions will require unforeseen repositioning or transfers among them as in the case of the retrieval of an accidentally released object. In this case, complex maneuvers are anticipated involving a variety of spacecraft that are not necessarily located at stable locations and thus have relative motion between each other.

This multivehicle environment poses new requirements for control and display of their relative positions. Conventional scenarios involve proximity operations between two vehicles only. In these two-spacecraft missions, the maneuver may be optimized and precomputed in advance of the time of the actual mission. However, since the variety of possible scenarios in a multivehicle environment is large, a future spacecraft environment could require astronauts to execute maneuvers that may not have been precomputed. This demand will require an on-site planning tool that allows the fast, interactive, informal creation of fuel-efficient maneuvers meeting all constraints set by safety rules.

The difficulties encountered in planning and executing orbital maneuvers originate from several causes.¹⁻³ First, the orbital motions are expressed and tend to be perceived in a coordinate frame attached to a large proximate vehicle such as the space station and, thus, represent relative rather than

absolute motions. The curved relative motion trajectories, resulting from maneuvering burns and the acting orbital mechanics forces, are counterintuitive and differ from common motion patterns experienced on Earth. This difficulty is compounded by the fact that a completed maneuver, which essentially is a timed orbital change, involves a potentially third-order or higher-order control process with departing, maneuvering, and braking thrusts. Even without considering the counterintuitive dynamics, these higher-order processes are difficult to control.⁴ Furthermore, the interaction between corrective thrust direction and magnitude on the one hand, and the time of arrival and resulting spacecraft position and velocity on the other is highly nonlinear, complicating iterative, manual efforts to drive a spacecraft to a desired stable position.

Second, the operation might involve targets that are not at a stable location and are drifting under the influence of orbital mechanics forces. This requires both the rendezvous position and the rendezvous time to be chosen in accordance with the target's anticipated relative motion trajectory.

Third, multivehicle orbital missions are subject to safety constraints, such as clearance from existing structures, allowable approach velocities, angles of departure and arrival, and maneuvering burn restrictions due to plume impingement or payload characteristics. Design of a fuel-efficient trajectory that satisfies these constraints is a nontrivial task.

It is clear that visualization of the relative trajectories and control forces in an easily interpretable graphical format will greatly improve the feel for orbital motions and control forces and provide direct feedback of the operators' control actions. Furthermore, visualization of the constraints in a pictorial format will enable interactive, graphical trajectory planning in which the design may be iteratively modified until all constraints are satisfied.

Typical in-plane maneuvers about a space station in LEO are the R-bar burn along the orbital radius vector and the V-bar burn along the orbital velocity vector. An outward R-bar burn (upward) will result in a relative trajectory in the backward direction, with a closed elliptical shape, which, after one orbit, will return the spacecraft to its original location. In contrast, a forward V-bar burn will result in an open trajectory, along which the spacecraft will initially move forward, but later on gain altitude and fall behind. After one orbit the spacecraft will have returned to the V-bar, 16,957 m behind

Received Feb. 1, 1991; revision received Dec. 10, 1991; accepted for publication March 22, 1992. Copyright © 1992 by the American Institute of Aeronautics and Astronautics, Inc. No copyright is asserted in the United States under Title 17, U.S. Code. The U.S. Government has a royalty-free license to exercise all rights under the copyright claimed herein for Governmental purposes. All other rights are reserved by the copyright owner.

*Senior Lecturer, Faculty of Aerospace Engineering; also National Research Council Senior Research Associate, NASA Ames Research Center, Moffett Field, CA 94035. Member AIAA.

†Group Leader, Advanced Displays and Spatial Perception, Aerospace Human Factors Research Division; also Research Staff Member, School of Optometry, University of California, Berkeley, CA 94720.

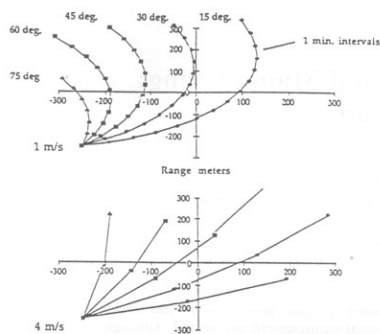


Fig. 1 Relative orbital trajectories for different thrust magnitudes (1 and 4 m/s) and angles measured upward from the +V-bar for an insertion point below the space station's orbit and behind its center of mass. The space station is located with its center of mass at the origin. Note that the effects of the orbital dynamics can be overpowered by increasing thrust at the cost of increased relative velocity that must be canceled for a successful rendezvous.

the original location, for a 1-m/s burn and 480-km circular orbit.

In general, a chasing vehicle's maneuvers in the orbital plane need not have solely V-bar or R-bar components but components of both. In addition, it may also have out-of-plane components. Furthermore, its initial position may not be stable, i.e., offset with respect to its target's V-bar, and the desired flight time may be a fraction of an orbital period, i.e., 10–20 min. Under these circumstances, the full effects of orbital dynamics are not given sufficient time to completely manifest themselves, but still are experienced as a kind of "variable orbital wind" blowing the controlled vehicle off a desired straight path. Figures 1 and 2 illustrate the kinds of deflections the "orbital wind" may produce for more generic maneuvers. In particular, Fig. 1 shows how the deflections caused by orbital dynamics can be partially overcome by using stronger thrusts. This brute force technique, however, can be very costly due to the fuel required for both departure and braking on arrival.

Limitations of Present Techniques

The present maneuvering techniques are well established and rely in most cases on visual contact and the use of a V- or R-bar reference in a crewman optical alignment sight (COAS).^{1,2} In a V-bar approach toward a target in the positive V-bar direction, the initial burn is made in a direction slightly depressed downward with respect to the V-bar. After a short while, the spacecraft will "ascend" again and cross the V-bar. At the V-bar crossing, a small downward R-burn is initiated, which again "depresses" the spacecraft below the V-bar. This process is repeated several times. The spacecraft thus proceeds along the V-bar in small "hops" until the target is reached. However, this technique is highly restricted, is not fuel-optimal, and may not conveniently satisfy other operational constraints of a multivehicle environment.

It is clear from the preceding examples that orbital motion can be complex, highly counterintuitive, and involve tightly interacting parameters. A burn toward the target might have an unintended opposite result. Relative motion is, in particular, difficult to visualize for a combined R-V-bar burn that has a component out of the orbital plane and that occurs at a nonstationary location off the V-bar. It is therefore very useful to graphically visualize the relative motion trajectories. Providing predictors on planning displays that foretell the final consequences of a maneuvering burn is, however, not sufficient symbolic enhancement to enable an operator to plan

a timed maneuver. The nonlinear interaction between thrust magnitude and direction, with time of arrival and final relative position and velocity, preclude tractable manual control over the position and time of the predictor's endpoint.

Orbital Maneuvers Planning System

Design Considerations

The purpose of the interactive orbital planning system is to enable the operator to design an efficient complex multiburn maneuver, subject to the stringent safety constraints of a future space station traffic environment. The constraints include clearances from structures, relative velocities between spacecraft, angles of departure and arrival, approach velocity, and plume impingement. The basic idea underlying the system is to present the maneuver as well as the relevant constraints in an easily interpretable pictorial format. This format does not just provide the operator with immediate visual feedback on the results of his design actions to enable him to meet the constraints on his flight path, but goes beyond conventional approaches by introducing geometric, symbolic, and dynamic enhancements that bring the intellectual demands of the design process within normal human capacity.^{1,3-9} The specific methods for enabling interactive trajectory design and visualization of constraints have been discussed in detail elsewhere and will not be repeated here.¹⁰⁻¹² Though the display also can handle planning out-of-plane maneuvers, the discussion will be limited to maneuvers in the orbital plane.

Example of a Three-Burn Maneuver

An illustrative example of an in-plane three-burn maneuver is shown schematically in Fig. 3. The trajectory originates from relative position *A* at time $t = t_0$ and is composed of two waypoints *B* and *C* that specify the location in space station coordinates at which the chaser spacecraft will pass at a given time. At a waypoint the orbital maneuvering system or other reaction control system can be activated, creating a thrust vector of a given magnitude for a given duration in a given direction, in or out of the orbital plane. The duration of the burn is considered to be very short in comparison with the total duration of the mission. In the orbital dynamics computations, this means that a maneuvering burn can be considered a velocity impulse that alters the direction and magnitude of the instantaneous orbital velocity vector of the spacecraft, inserting it into a new orbit.

Since the initial location *A* is not necessarily a stationary point, the magnitude and direction of the relative velocity of the chaser at point *A* are determined by the parameters of its orbit. If no maneuvering burn were initiated at $t = t_0$, the chaser would continue to follow the relative trajectory 1, subject to the parameters of its original orbit; see the dotted line in Fig. 3. However, a maneuvering burn at $t = t_0$ will alter

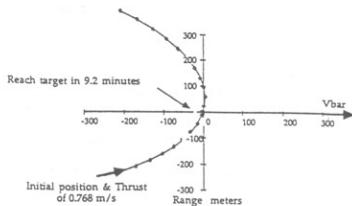


Fig. 2 Rendezvous initiated by control of thrust and direction of a maneuvering burn, i.e., the forward method. By using a planning tool that provides a forward predictor of the effects of a planned maneuvering burn, a subject can find by trial and error a combination of thrust and insertion angle that will produce a trajectory to return to the space station from an offset position. Planning for a particular arrival time or selecting a fuel-optimal maneuver is, however, manually very difficult, with only a forward predictor to assist the operator.

the original orbit so that the chaser will follow the relative trajectory 2, subject to the parameters of this new orbit.

In Figure 3 v_1 and v_2 indicate the relative velocity vector of the chaser just before and after the maneuvering burn, respectively, where v_1 and v_2 are tangential to the relative trajectories 1 and 2, respectively. The vector difference between v_1 and v_2 , v_a , is the velocity vector change initiated by the burn and corresponds to the direction and magnitude or duration at which the orbital maneuvering system is activated. Likewise, at waypoint B the burn v_3 alters the orbit from orbit 2 to orbit 3.

Location C is the terminal waypoint and is in this case the location where the target will arrive at the final time t_f . Since the target has an orbit of its own, orbit 4, it will have a terminal relative velocity vector v_a at $t = t_f$. The relative velocity between target and chaser is the vector difference between v_3 and v_a . This vector determines the retro-burn that is needed at the target location to bring the relative velocity between chaser and target to the minimum required for the docking operation.

Inverse Method of Solving Orbital Motion

Interactive trajectory design demands that the operator be given free control over the positioning of waypoints. However, the usual input variables of the equations of orbital motion are the magnitude and direction of the burn, rather than the time and relative position of waypoints. Since it is difficult to control the positioning of waypoints by these usual inputs, an "inverse method" is required to compute the values of a burn necessary to arrive at a given waypoint positioned in time and space by the operator. This method is outlined here.

The orbital motion can be computed from its momentary position and velocities, relative to a reference spacecraft with a known circular orbit.^{10,11,13-15} Thus, for a given initial relative position A with $x(t_0)$ and an initial relative velocity $v(t_0)$ at $t = t_0$, the relative position and velocities of a waypoint at time $t = t_1$ can be computed. However, a maneuvering burn at $t = t_0$ will cause a change in the direction and magnitude of the relative velocity vector $v(t_0)$. As a result of this maneuvering burn, the position of the waypoint at time t_1 will change as well.

Consider v_a and α_a to be the magnitude and direction of the velocity change due to the maneuvering burn. Then the relative position and velocity at $t = t_1$, $x(t_1)$, will be a complex nonlinear function of v_a and α_a ,^{10,11} hereafter referred to as the "forward" solution. Consider now that the operator is given direct control over v_a and α_a by slaving these variables, respectively, to the x and y motions of a controller such as a joystick or tracking ball. A controller command in either the x or y direction will result in a complex nonlinear motion pattern of $x(t_1)$. Furthermore, this motion pattern will change with the initial conditions. This arrangement is highly undesirable in an interactive trajectory design process in which the operator must have direct, unconstrained, and intuitive control over the positioning of waypoints.

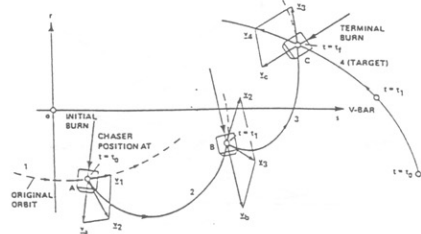


Fig. 3 Example of a three-burn maneuver. Relative trajectories are altered by maneuvering burns. The final burn v_c brings the relative velocity between chaser and target to zero.

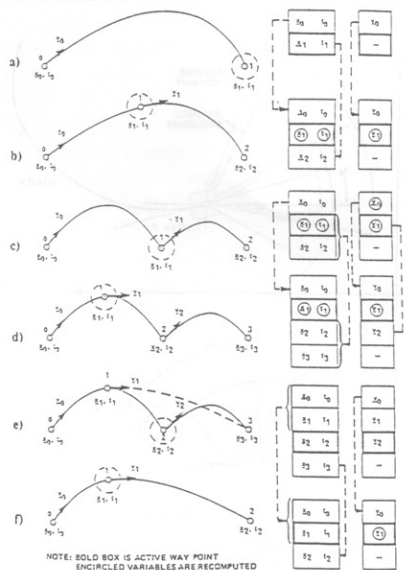


Fig. 4 Editing of waypoints. The waypoint stack is altered by creating, changing, or deleting waypoints. The active waypoint parameters are in the boldly drawn box.

It is therefore essential to give the operator direct control over the position and relative time of waypoints, rather than the magnitude and direction of the burn. The inverse method by which this is accomplished computes the magnitude and direction of the burn required to bring the spacecraft from initial location $x(t_0)$ to the waypoint $x(t_1)$ at $t = t_1$. This inverse technique contrasts with conventional display aids for proximity operations that are generally forward looking and provide a predictor.^{6,7} Although forward-looking displays are probably well suited as flying aids for real-time, out-the-window control, a planning system need not conform to this style of aiding. A Newton-Raphson iterative scheme has been employed for computing the inverse solution.^{10,11} However, for small deviations from near-circular orbit, the relative motion between two co-orbiting spacecraft in close proximity can be simplified by a first-order approximation, which allows simple closed-form solutions both for the forward and inverse problem, known as the Clohessy-Wiltshire equations¹⁶ or the Euler-Hill equations.¹⁷⁻¹⁹

Active Waypoint Concept

Although a trajectory may be composed of several waypoints, only one waypoint at a time, the active waypoint, is controlled by the operator. Although the position and time of arrival (TOA) of the active waypoint can be varied, the position and time of arrival of all other waypoints remain unchanged. However, variations in the active waypoint will cause changes in the trajectory sections and waypoint maneuvering burns just preceding and just following the active waypoint. The on-line solution of the inverse algorithm enables these changes to be visualized almost instantaneously and provides the operator with on-line feedback on his design actions. In the display three modes for changing the parameters of the active waypoint were adapted: 1) "unlocked" posi-

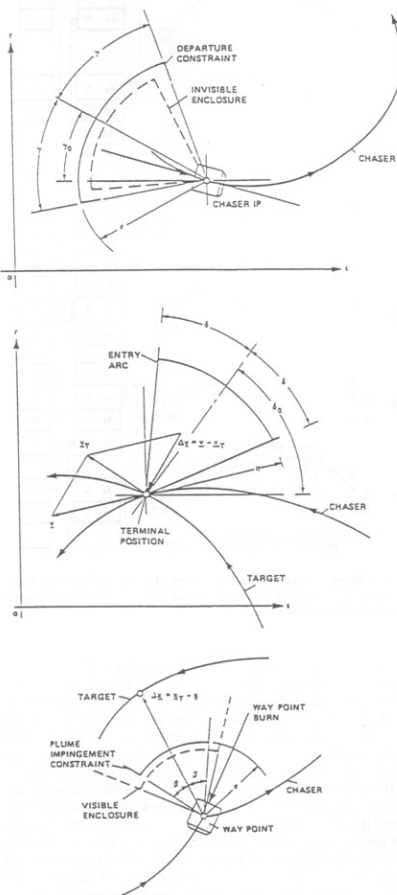


Fig. 5 Visualization of operational constraints. Angular and magnitude constraints on maneuvering thrusts at departure (top), at arrival (middle), and on plume impingement during the maneuver (bottom).

tioning mode, in which the waypoint can be moved around freely in three-dimensional space while its TOA remains fixed; 2) "locked" position mode, in which only its TOA is changed; and 3) "locked-on-trajectory" mode, in which the waypoint is moved along the unpowered trajectory of its neighboring waypoints by changing its TOA. In the last case, the waypoint is unpowered. This mode is useful in particular for first-time positioning of intermediate waypoints and for checking whether operational constraints, such as approach velocity constraints, are violated.

Waypoint Editing

The trajectory design process involves changes in existing waypoints, addition of new points, or deletion of existing undesired points. An illustrative example of this waypoint editing process is shown in Fig. 4. The waypoints are most con-

veniently managed by a waypoint stack, which includes an up-to-date sequential list of the waypoint data. Similar to a spreadsheet, the waypoint stack allows modification, addition, or deletion of "cells," while at all times satisfying the boundary conditions with neighboring cells. Each cell includes the position x , time of arrival t , and relative velocity v , just after initiating the burn, of a given waypoint. The method by which the waypoint stack is managed is described next.

Figure 4a shows two waypoints: the initial point x_0 and terminal point x_1 . The initial waypoint is defined by the initial conditions of the situation and cannot be activated or changed by the operator. The terminal waypoint x_1 is thus the active waypoint that can be changed and placed at a required location. The corresponding waypoint stack is shown on the right. The active waypoint box is drawn in bold. The relative velocity stack shows only the velocity v_0 , which is the relative velocity just after the burn at waypoint 0, computed by the inverse algorithm and required to reach point x_1 at time t_1 .

Figure 4b shows the addition of a new waypoint. Although its time of occurrence may be manually adjusted later, the new waypoint is at first added halfway in time on the trajectory section just preceding the active waypoint. Thus, its time of arrival is chosen to be $t = 0.5(t_1 + t_0)$, where i is in this case 1 and relates to the stack before modification. The new position x_1 and relative velocity v_1 are computed by a conventional "forward" method, by computing the relative position at the new time t_1 , using the existing orbital parameters previously computed with x_0 , v_0 , and t_0 . The newly computed waypoint position, time, and relative velocity are inserted between points 0 and 1 of the stack before modification and the new waypoint is chosen to be the active one. The dotted lines in Fig. 4 indicate variables that are transferred without modification and the encircled variables are the newly computed ones. It is important to note that since the relative velocity vectors v_0 and v_1 are matched to the required waypoints x_1 and x_2 , respectively, the inverse algorithm does not need to make any adjustments.

Figure 4c shows the results of changes in the newly created waypoint on the waypoint stack. Since x_1 and t_1 are varied, the relative velocity at waypoint 0, v_0 , will be readjusted by the inverse algorithm and likewise the relative velocity v_1 .

Figure 4d shows the creation of an additional new waypoint. Since the active waypoint prior to the addition was point 1, the new point is added halfway between points 0 and 1 and its position and relative velocity are computed with the forward method. The new values are inserted between points 0 and 1 of the stack before modification and the new waypoint is again set to be the active one.

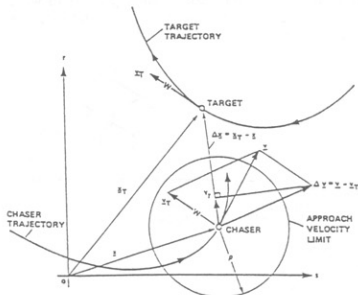


Fig. 6 Approach velocity constraint limit circle. The allowable approach velocity is considered to be proportional to the range to the target so that when the constraint is defined, allowable relative velocity decreases as the target is approached. If the target is contained within the circle, the approach velocity constraint has been exceeded.

In Fig. 4e waypoint 2 is activated. Apart from the shift in active waypoint, the stack remains unchanged. The dotted line shows the direct-path section between points 1 and 3 without the intermediate burn at point 2. Deletion of the waypoint 2 will remove this point from the stack and after that close the gap; see Fig. 4f. However, v_1 has to be readjusted to fit the new direct-path section. This adjustment is made on-line by the inverse algorithm.

The repetitive use of the inverse algorithm to calculate the trajectories linking each triad of waypoints presents the planner with a kind of "geometric spreadsheet" that preserves certain relationships between points in space, namely, that they are connected by unpowered (coasting) trajectories for their particular separation in time, whereas their other properties, namely, their relative position in space, may be freely varied. To the best of our knowledge, this application of inverse dynamics to such a display problem is new and has some very helpful side effects. The continuously active background computation to preserve the relative position and time of each waypoint creates an illusion of an inertially stable space that assists planning of relative movements about a target spacecraft. Since changes in the relative position and time of a waypoint only propagate to adjacent trajectory sections and maneuvering burns, this technique assists planning by allowing, to some extent, separable solutions to the plume impingement, velocity limit, and traffic conflict problems. For instance, once a waypoint has been positioned immediately after departure to bring departure velocities within prescribed limits, subsequent waypoints can be positioned freely. For instance, additional burns can be inserted to clear a structure, without disturbing the earlier solution found for the departure constraint. Likewise, the effect of adjustments of a waypoint positioned immediately before rendezvous to satisfy the terminal situation can be isolated from the effect of adjustments in preceding waypoints. This isolation of the solutions of the separate problems is an essential characteristic since without it, the solution to one aspect of the maneuver problem would undo a solution to another.

Operational Constraints

The multispacecraft environment will require strict safety rules regarding clearance from existing structures. Thus, spatial "envelopes" through which a spacecraft is not allowed to pass can be visualized on the display by the construction of graphic icons whose shape and dynamic behavior inform the planner which flight rules are violated and what actions need to be taken to satisfy them.

Restrictions on angles of departure and arrival may originate from structural constraints at the departure gate or the orientation of the docking gate or grapple device at the target craft. Limits for the allowable angles of departure or arrival can be visualized as bracketed arcs or cones on the display; see the top and middle of Fig. 5. In addition, the magnitude of the terminal approach velocity at the target might be limited by the target characteristics. Limits for the allowable start and end velocities can be visualized as limit arcs associated with the approach or departure cones. The limit arc symbols shown in Fig. 5 graphically indicate allowable ranges of magnitude and direction for thrusts and relative velocities. Three levels of display are considered. If the burn vector is not enclosed within the solid arc (the top of Fig. 5), the arc is drawn brightly yellow to indicate that the constraint has been violated. On the other hand, if the burn vector is within the dotted enclosure, the departure burn is well within the prescribed limits, and the departure arc is not shown. In all other cases, the arc is drawn dimly yellow to indicate that it is close to being violated.

Waypoint maneuvering burns are subject to plume impingement constraints. Hot exhaust gases of the orbital maneuvering systems may damage the reflecting surfaces of sensitive optical equipment such as telescopes or infrared sensors. Even cold nitrogen jets might disturb the attitude of the target sat-

ellite. Maneuvering burns toward this equipment are restricted in direction and magnitude, where limits for the allowable direction and magnitude are a function of the distance to the equipment and plume characteristics. These limits can be visualized as bracketed limit arcs on the display; see the bottom of Fig. 5. If the burn vector does intersect the solid arc, it is drawn brightly yellow to indicate that the plume impingement constraint is violated. Similar to the departure constraint, if the burn vector does not intersect the dotted arc, it is well within limits and the arc is not shown, and for all other cases, it is drawn dimly yellow.

Flight safety requires that the relative velocity between spacecraft is subject to approach velocity limits. In conventional docking procedures, this limit was proportional to the range.^{1,2} A previously used rule of thumb is to limit the relative approach velocity to 0.1% of the range. This conventional rule is quite conservative and originates from visual procedures in which large safety margins are taken into account to correct for human or system errors. Although the future traffic environment will be more complex and therefore demand large safety margins, more advanced and reliable measurement and control systems may somewhat relax these demands.

In this display the relative approach velocity is defined as the component of the relative approach velocity vector between the two spacecraft along their mutual line of sight; see Fig. 6. The limit on this relative approach velocity is a function of the range between the spacecraft. This function will depend on the environment, the task and reliability of measurement and control equipment and cannot be determined at this stage. For this display a simple proportional relation has been chosen. The approach velocity limit is visualized on the display as a circle drawn around the chaser indicating the minimum range between the two spacecraft allowed for the present approach velocity; see Fig. 6. If the target craft appears within this circle, the approach limit has been violated.

Discussion

The proposed interactive orbital planning system constitutes a preliminary attempt to determine a display format that may be useful in a future dense spacecraft traffic environment. The examples shown deal with the most general situation, which involves departures from or arrival at nonstationary locations. Such missions may represent worst-case situations, but these are the ones most likely to require customized maneuvering.

The basic principle of graphical-interactive planning could be extended to other problems involving tightly coupled variables and complex situation-dependent constraints, such as terminal air-traffic control, fuel-efficient aircraft flight-path planning, the path planning of a remotely controlled terrain vehicle, e.g., the Mars rover, or the planning of "gestures" for robot manipulators. The "geometric spreadsheet" approach will allow solution by an iterative sequence of simple independent steps.

The constraints considered encompass in a broad sense the general type of restrictions that are expected in the multivehicle environment, e.g., limitations on departure and approach velocities, plume impingement, and clearance from structures. The basic principle of the graphical-interactive visualization of constraints can be used for visualizing other task-related state variables, control functions, and restrictions as well.

In the present display, only pure impulse maneuvering burns are considered, in which the duration of the burn is negligible with respect to the duration of the mission and these burns cause major changes in the relative trajectories. Station-keeping or fly-by missions, however, require a more sustained type of activation, such as periodic small burns with several-second intervals over a time span of several minutes. A more "distributed" way of activating the orbital maneuvering system could be introduced in which the burn profile is computed in the background for carrying out certain fly-by or station-keeping missions requested by the operator. Visualization and

activation of this type of control should follow guidelines similar to those used in the present display.

Trivial and repetitive actions such as the the optimal positioning of a local waypoint to clear a spatial constraint, or satisfy departure constraints, could very well be automatically performed by the system. This possibility calls for the need to introduce partially automated design steps that unburden the operator from unnecessary actions and might speed up the design process. A design criterion for these automated actions is that they should be performed within several seconds after the operator's request. The described display will be useful in fully automated design procedures as well, if such procedures are at least one order of magnitude faster than the operator performing the action manually. In this case, the display will allow the operator to review and edit the automated design quickly and request corrective action, if unique mission features or failures demand it.

References

- ¹NASA, *Flight Procedures Handbook*, NASA Johnson Space Center, JSC-10566, Nov. 1982.
- ²NASA, *Rendezvous/Proximity Operations Workbook*, NASA Johnson Space Center, RNDZ 2102, 1983.
- ³Allen, J. P., "Physics at the Edge of the Earth," *Pictorial Communication in Virtual and Real Environments*, edited by S. R. Ellis, M. Kaiser, and A. Grunwald, Taylor and Francis, London, 1991, pp. 12-21.
- ⁴Wickens, C. D., "The Effects of Control Dynamics on Performance," *Handbook of Perception and Human Performance*, edited by K. R. Boff, L. Kaufman, and J. P. Thomas, Wiley, New York, 1986, Vol. II, pp. 3g-1, 39-60.
- ⁵Palmer, E., Jago, S., Baty, D., and O'Connor, S., "Perception of Horizontal Aircraft Separation on Cockpit Display of Traffic Information," *Human Factors*, Vol. 22, No. 5, 1980, pp. 605-620.
- ⁶McCoy, W. K., Jr., and Frost, G. G., "Predictor Display Techniques for On-Board Trajectory Optimization of Rendezvous Maneu-

vers," Aerospace Medical Research Labs., Wright-Patterson AFB, OH, AMRL-TR-66-60, May 1966.

⁷Brody, A. R., "A Forward-Looking Interactive Orbital Trajectory Plotting Tool for Use with Proximity Operations," NASA CR 177490, June 1988.

⁸Eyles, D., "A Computer Graphics System for Visualizing Spacecraft in Orbit," *Pictorial Communication in Virtual and Real Environments*, edited by S. R. Ellis, M. Kaiser, and A. Grunwald, Taylor and Francis, London, 1991, pp. 196-206.

⁹Ellis, S., McGreevy, M. W., and Hitchcock, R., "Perspective Traffic Display Format and Airline Pilot Traffic Avoidance," *Human Factors*, Vol. 29, No. 4, 1987, pp. 371-382.

¹⁰Grunwald, A. J., and Ellis, S. R., "Interactive Orbital Proximity Operations Planning System," *Proceedings of the 1988 IEEE International Conference on Systems, Man, and Cybernetics* (Peking, China), IEEE CAT 88CH2556-9, Aug. 1988, pp. 1305-1312.

¹¹Grunwald, A. J., and Ellis, S. R., "Interactive Orbital Proximity Operations Planning System," NASA TP 2839, Nov. 1988.

¹²Grunwald, A. J., and Ellis, S. R., "Design and Evaluation of a Visual Display Aid for Orbital Maneuvering," *Pictorial Communication in Virtual and Real Environments*, edited by S. R. Ellis, M. Kaiser, and A. Grunwald, Taylor and Francis, London, 1991, pp. 207-231.

¹³Kovalevsky, J., *Introduction to Celestial Mechanics*, translated by Express Translation Service, Springer-Verlag, New York, 1967, pp. 1-19.

¹⁴Taff, L. G., *Celestial Mechanics, a Computational Guide for the Practitioner*, Wiley, New York, 1985.

¹⁵Thomson, W. T., *Introduction to Space Dynamics*, Dover, New York, 1986.

¹⁶Clohesy, W. H., and Wiltshire, R. S., "Terminal Guidance System for Satellite Rendezvous," *Journal of the Aerospace Sciences*, Vol. 27, No. 9, 1960, pp. 653-658, 674.

¹⁷Wheelon, A. D., "Midcourse and Terminal Guidance," *Space Technology*, edited by H. Seifert, Wiley, New York, 1959, pp. 26-32.

¹⁸Hill, G. W., "Research in Lunar Theory," *American Journal of Mathematics*, Vol. 1, No. 1, 1878, pp. 5-26.

¹⁹Kaplan, M. H., *Modern Spacecraft Dynamics & Control*, Wiley, New York, 1976, pp. 108-115.

Visual Display Aid for Orbital Maneuvering: Experimental Evaluation

Arthur J. Grunwald*

Technion—Israel Institute of Technology, Haifa 32000, Israel
and

Stephen R. Ellist

NASA Ames Research Center, Moffett Field, California 94035

An interactive proximity operations planning system, which allows on-site planning of fuel-efficient, multi-burn maneuvers in a potential multispacecraft environment, has been experimentally evaluated. An experiment has been carried out in which nonastronaut operators with brief initial training were required to plan a trajectory to retrieve an object accidentally separated from a dual-keel Space Station, for a variety of different orbital situations. The experiments have shown that these operators were able to plan workable trajectories, satisfying a number of operational constraints. Fuel use and planning time were strongly correlated, both with the angle at which the object was separated and with the existence of spatial constraints. Planning behavior was found to be strongly operator-dependent. This finding calls for the need for standardizing planning strategies through operator training or the use of semiautomated planning schemes.

Introduction

THE proximate orbital environment of future spacecraft in low Earth orbit (LEO) may include a variety of spacecraft co-orbiting in close vicinity. Most of these spacecraft will be "parked" in a stable location with respect to each other, i.e., they will be on the same circular orbit. However, some missions will require unforeseen repositioning or transfers among them, as in the case of the retrieval of an accidentally released object. In this case, complex maneuvers are anticipated involving a variety of spacecraft that are not necessarily located at stable locations and thus have relative motion between each other. Furthermore, these types of maneuvers will have to meet stringent safety constraints, such as clearances from structures, restrictions concerning allowable departure and arrival velocities and angles, or plume impingement constraints.

The interactive proximity operations planning tool, in detail described in Refs. 1-4, enables the operator to deal with the highly complex and counterintuitive orbital situation by allowing him direct control over trajectory waypoints through an "inverse dynamics" algorithm and by enabling him to plan the trajectory through an iterative sequence of relatively simple independent solutions. Central in the trajectory planning process is the immediate visual feedback of trajectory shapes and operational constraints, provided by the continuously active background computation, transparent to the user.

This paper deals with the interaction of nonastronaut, but nonetheless highly professional operators (airline pilots, aerospace scientists), with the planning tool. It was of particular interest to investigate whether they could be familiarized quickly with orbital motions and complex orbital maneuvering, and whether they could plan workable trajectories, satis-

fying all operational constraints, within the reasonable time frame of several minutes. It was also of interest to investigate the variability in planning strategies of the various operators. In view of the considerable freedom left to the operator in the planning process, a large variability is expected. Although practice should reduce the variability for each operator individually as she gradually crystallizes her design strategy, it is far from certain whether all operator strategies will lead to the same solutions. The results of these experiments form the guideline for continued display developments, such as the inclusion of partially or fully automated optimization schemes, or standardization of training procedures.

Experimental Study

Purpose of the Study

An experimental study has been carried out to evaluate the operator's performance envelope while using the proximity operations planning tool. The purpose of this study was 1) to determine the time frame, after initial training of the operator,

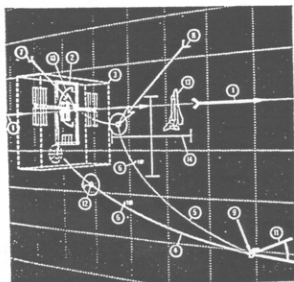


Fig. 1 Screen image of the main viewpoint of the proximity operations planning tool showing an incompletely planned mission for which three burns have been selected. The velocity vector or $+Y$ -bar is depicted by the arrows (1) pointing to the right on the central grid line. Note that the relative velocity vector on arrival, shown by the arrow (2) in the lower right of the viewport, is outside of the entry cone (11), indicating the acceptable range of relative velocity on arrival with the target craft.

Received May 5, 1991; revision received Dec. 10, 1991; accepted for publication March 23, 1992. Copyright © 1992 by the American Institute of Aeronautics and Astronautics, Inc. No copyright is asserted in the United States under Title 17, U.S. Code. The U.S. Government has a royalty-free license to exercise all rights under the copyright claimed herein for Governmental purposes. All other rights are reserved by the copyright owner.

*Senior Lecturer, Faculty of Aero-Space Engineering; also National Research Council Senior Research Associate, NASA Ames Research Center, 1985-1987, Moffett Field, CA 94035. Member AIAA.

†Group Leader, Aero-Space Human Factors Research Division, Advanced Displays and Spatial Perception; also Staff Member, School of Optometry, University of California, Berkeley, CA 94720.

Table 1 Subject planning performance; subjects are instructed to minimize either fuel use f or planning time t

Subject	Instruction (t or f)	Planning time (s)	Fuel use (m/s)	Regression multiple correlation of fuel use vs violation score (R^2)
DB	t	526	3.966	0.214
ED	t	182	3.666	0.190
LK	t	572	5.602	0.403
RE	t	362	2.872	0.188
AJ	f	179	2.974	0.250
RO	f	317	4.764	0.379
SB	f	265	2.890	0.136
Average subject	t group	411	4.027	0.339
Average subject	f group	254	3.543	0.319
Average subject	both groups	343	3.820	0.349

$df = 86$.

All multiple correlations are significant at least at the $p < 0.01$ level.

necessary for carrying out a planning mission, randomly chosen from a broad spectrum of orbital situations; 2) to determine the factors that influence the operator's planning time, i.e., initial orbital situation, constraints; 3) to determine whether and to what extent the operator is able to optimize orbital fuel expenditure and determine the factors that influence the fuel use; 4) to investigate whether a tradeoff exists in operator performance between fuel use and planning time; 5) to investigate whether specific subject instruction to minimize either the planning time or fuel use affects this tradeoff; and 6) to identify planning strategies and determine the variability in the subject's planning performance.

Description and Design of the Experiment

The experiment was carried out on a Silicon Graphics IRIS 2400 workstation and the subjects interfaced with the system through a mouse and "soft" control buttons, programmed on the display. The experiment simulated the planning of a proximity operations retrieval mission of an object inadvertently released from a variety of positions along the main structures of a dual-keel Space Station configuration, in low 480-km altitude circular earth orbit. The chasing vehicle for the maneuver departed from a +V-bar location on the station and may be thought of as a craft attempting to recover an astronaut or object accidentally released with either zero or moderate (1.0 m/s) separation velocity v and that is drifting away under the influence of orbital mechanics forces. Out-of-plane separation velocity components of the target were randomly selected to be ± 0.25 or ± 0.5 m/s. The in-plane direction of the separation velocity vector v at release was randomly selected from eight possible directions, spaced in 45-deg intervals, about the +V-bar. The 10 possible orbital insertion points for the targets were distributed along the port keel of the Space Station from 200 m above the center of mass to 150 m below it and were also selected randomly to produce a total of 90 different recovery scenarios. The planned one-way flight time was 20 min and the maneuver took place during orbital daylight.

Description of the Task

The subject's task was to expeditiously plan a three-dimensional trajectory from a Space Station +V-bar departure port to rendezvous with the target, subject to departure and plume impingement constraints on the station, avoidance of the station's structure, and alignment of the relative velocity vector on rendezvous to fit within a 30-deg entrance cone. Such restrictions on the angles of departure and arrival might originate from structural constraints at the departure gate, or the orientation of the docking gate or grapple device at the target craft. Subjects were divided in two groups: the first group was instructed to minimize the fuel use, while keeping the planning

time within acceptable limits; the second group was instructed to complete its planning task quickly (much as one would wish to walk across a room without wasting time), and not to worry about minimizing overall fuel use, although each subject was limited to a total velocity impulse v of 12-m/s maneuvering fuel.

Figure 1 illustrates a three-burn partial solution to one of the experimental scenarios. The main window shows the orbital plane with the orbital flight vector (1), the Space Station (2) with its spatial constraint envelope (3), target trajectory (4) and chaser trajectory (5), both with time markers (6) indicating the time in minutes after initiating the maneuver. Departure burn (7), intermediate burn (8), and retro burn at the target (9) are indicated by vectors, of which the length depicts the magnitude of the burn. Departure constraints are visualized by the bracketed arc (10) and arrival constraints by the approach cone (11). Both the departure arc and entrance cone

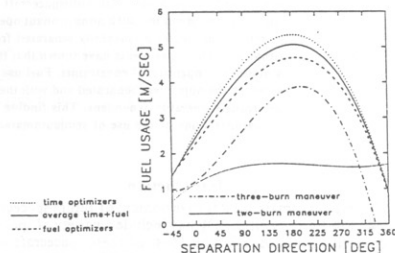


Fig. 2a Third-order regression curves for fuel usage vs target separation velocity vector direction. Analytical results of fuel usage for two- and three-burn maneuvers are also shown.

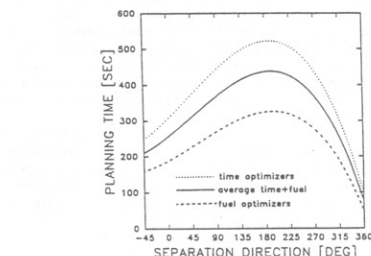


Fig. 2b Third-order regression curves for planning time vs target separation velocity vector direction.

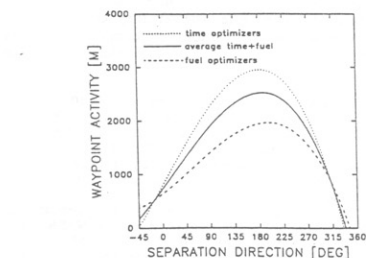


Fig. 2c Third-order regression curves for in-plane integrated waypoint displacement (m) vs target separation velocity vector direction.

Table 2 Correlation values (R^2) of third-order regression curves of separate direction vs fuel usage, vs planning time, and vs waypoint activity for the individual subjects

Subject	Instruction (t or f)	Regression multiple correlation of fuel use vs separate direction (R^2)	Regression multiple correlation of planning time vs separate direction (R^2)	Regression multiple correlation of waypoint activity vs separate direction (R^2)
DB	t	0.558	0.125	0.124
ED	t	0.285	0.054*	0.104
LK	t	0.297	0.023 ns	0.143
RE	t	0.531	0.007 ns	0.036 ns
AJ	f	0.452	0.070*	0.139
RO	f	0.269	0.150	0.120
SB	f	0.549	0.056*	0.096
Average subject	t group	0.524	0.094	0.231
Average subject	f group	0.493	0.124	0.146
Average subject	both groups	0.539	0.131	0.268

df = 86.

*Significant at the $p < 0.05$ level.

ns = not significant.

All others are significant at the $p < 0.01$ level.

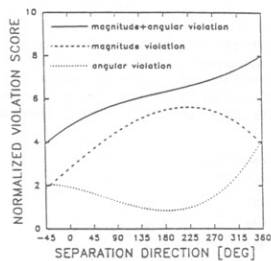


Fig. 3 Analytical results of third-order regression curves of violation scores vs the target separation velocity vector direction for a three-burn maneuver. The normalized magnitude violation curve shows a distinct maximum at the 225-deg separation angle, whereas the curve for the normalized angular violation score shows a minimum at 180 deg. The scores cannot be added and the magnitude violation is taken as the representative score.

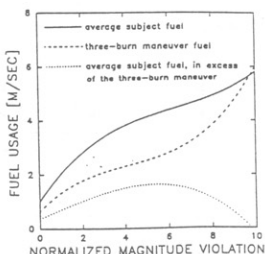


Fig. 4 Third-order regression curve of averaged-subject fuel use vs normalized magnitude violation score. The upward slope indicates that fuel use can be predicted from the violation score. The figure also shows the analytical regression curve for three-burn maneuver fuel use and the regression curve for the difference between the averaged-subject fuel use and 3-burn maneuver fuel use.

are drawn here brightly to indicate that departure and arrival velocity vectors have not yet been adjusted to fit the required constraints. Additional display attributes are the position of the target at intermediate waypoint time (12), additional vehicles like the orbiter (13), and a reference reticle in the center of the display (14).

Subject Background and Training

Seven subjects participated in the experiment. Three of them (ED, RE, RO) were airline pilots (DC-8, Boeing 737, P2, P5) of age 51–55 with 12,500–23,000 h of flight experience. One subject (DB) (age 54) was a retired navy pilot (A-4) with 5000 h of flight experience. The three remaining subjects (AJ, LK, SB) were nonpilot aerospace scientists aged 35–43. None of them, except two subjects (AJ, ED), were familiar with orbital operations and mechanics. Before beginning the experiment, the subjects carried out two 3-h training sessions usually completed in 1 day, in which they reviewed a training manual that interactively familiarized them with orbital mechanics and the various functions of the planning system. Finally, the manual guided them through a sample rendezvous planning mission in order to practice the display's controls and its operation.

Experimental Procedure

Data collection took about 8 hours and was generally spread across two days. Subjects were automatically presented through a UNIX C-shell script with the 90 rendezvous problems in four approximately equal groups of randomly ordered conditions. The following descriptive statistics were collected automatically by the IRIS computer: 1) planning time, 2) fuel use, 3) total number of way-points used, 4) operator activity such as number and type of operations and integral scores on the motion of waypoints in the planning process, and 5) a detailed account of constraint violations in the process, if any.

Results

Effect of Subject Instruction

Table 1 summarizes the average planning time and fuel use for 90 rendezvous planning missions, for each one of the subjects. The results show large variability between subjects. The subjects instructed to minimize fuel f on the account of planning time did not show significantly smaller fuel use [$F(1, 5) = 0.324$ $p < 0.594$] and those instructed to minimize the planning time t , did not have significantly shorter planning times, e.g., see RO and LK [$F(1, 5) = 2.033$ $p < 0.213$]. This indicates that the effect of subject instruction is highly masked by strong differences in basic planning strategy between the

subjects. Table 1 also shows the average subject performance for the t group, f group, and both groups.

Effect of Target Separation Parameters

Target separation parameters include the location of target separation above or below the V-bar, and the magnitude and direction of the separation velocity vector direction.

Anova analysis revealed significant effects of separation location and separation velocity vector direction on fuel use, ($F=4.689$, $df=9,45$, $p<0.001$) and ($F=49.891$, $df=7,35$, $p<0.001$), respectively. Since large individual differences in performance were found, it was preferable to describe these and other results by subject-to-subject regression analysis, presented here. Figures 2a-c show third-order regression curves for fuel use, planning time, and in-plane integrated waypoint displacement (in m) vs target separation velocity vector direction, where the angle is measured positive in the upward direction from the positive V-bar direction. The average subject curves for a particular group, i.e., t , f , or both, are the regressions for a set of 90 values, obtained by averaging each one of the 90 rendezvous scenarios across the subjects in each group. Multiple correlation values for each one of the regressions are listed in Table 2. All curves show clear maxima about the 180-deg angle, i.e., objects released in the backward or negative V-bar direction. For target separation in this direction, the spacecraft will move initially backward and downward with respect to the Space Station. An attempted two-burn maneuver to recover the target craft will result in the chaser passing right through the Space Station spatial constraint envelope [attribute (3) in Fig. 1]. In order to avoid the envelope, a third intermediate burn is needed. The intermediate waypoint can be placed such that the trajectory passes

either above or below the Space Station. Although the spatial constraints are satisfied, other constraints such as departure, arrival, plume impingement, and approach velocity constraints still have to be resolved. Figure 2a also shows analytical results of fuel use vs the separation velocity vector direction for two- and three-burn maneuvers. The location and time of arrival of the intermediate waypoint are chosen such that the trajectory just clears the envelope with minimum fuel cost. The minimum is empirically found to be unique. Although the fuel cost curve for the two-burn maneuver is almost flat, the curve for the three-burn maneuver shows a distinct maximum at about 180 deg. The difference between the curves can be attributed to the extra fuel cost involved in avoiding the Space Station envelope.

Figure 2a also shows that the average subject regression curves for the fuel usage, for the t , f , and both groups, are shifted upward with respect to the curve for the three-burn maneuver by a constant amount of 1 m/s. This indicates that the additional fuel needed to resolve the remaining constraint violations is independent of the target separation angle. The fuel use with the fuel optimizers is somewhat lower than that of the time optimizers.

A pronounced maximum at the 180-deg target separation velocity vector direction also appears in the regression curves for the planning time; see Fig. 2b. Surprisingly, the curve for the fuel optimizers is somewhat below that for the time optimizers, which indicates that instruction did not affect their absolute planning behavior. The strong increase in planning time for targets released in the backward direction can be attributed to both the time needed to position the third waypoint for clearing the structure, and the extra time needed to resolve other constraint violations resulting from this third

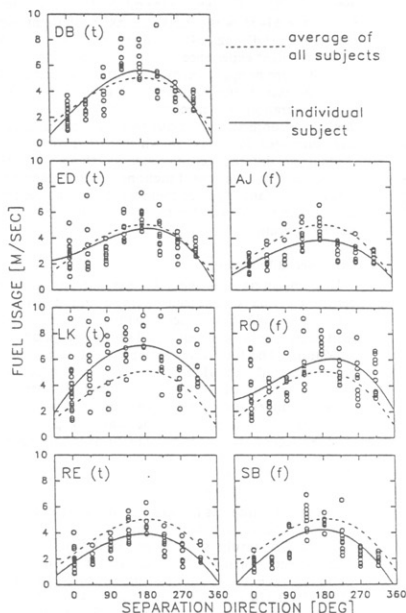


Fig. 5a Comparison of individual subject performance with performance, averaged over all subjects; third-order regression curves of fuel usage vs target separation velocity vector direction.

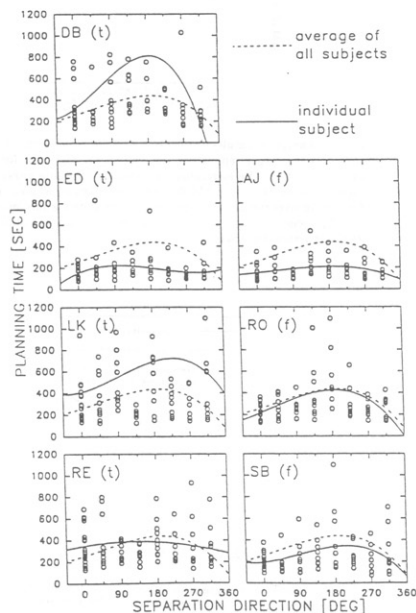


Fig. 5b Comparison of individual subject performance with performance, averaged over all subjects; third-order regression curves of planning time vs target separation velocity vector direction.

Table 2 Correlation values (R^2) of third-order regression curves of separate direction vs fuel usage, vs planning time, and vs waypoint activity for the individual subjects

Subject	Instruction (t or f)	Regression multiple correlation of fuel use vs separate direction (R^2)	Regression multiple correlation of planning time vs separate direction (R^2)	Regression multiple correlation of waypoint activity vs separate direction (R^2)
DB	t	0.558	0.125	0.124
ED	t	0.285	0.054 ^a	0.104
LK	t	0.297	0.023 ns	0.143
RE	t	0.531	0.007 ns	0.036 ns
AJ	f	0.452	0.070 ^a	0.139
RO	f	0.269	0.150	0.120
SB	f	0.549	0.056 ^a	0.096
Average subject	t group	0.524	0.094	0.231
Average subject	f group	0.493	0.124	0.146
Average subject	both groups	0.539	0.131	0.268

df = 86.

^aSignificant at the $p < 0.05$ level.

ns = not significant.

All others are significant at the $p < 0.01$ level.

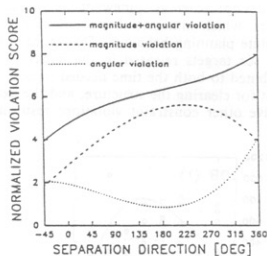


Fig. 3 Analytical results of third-order regression curves of violation scores vs the target separation velocity vector direction for a three-burn maneuver. The normalized magnitude violation curve shows a distinct maximum at the 225-deg separation angle, whereas the curve for the normalized angular violation score shows a minimum at 180 deg. The scores cannot be added and the magnitude violation is taken as the representative score.

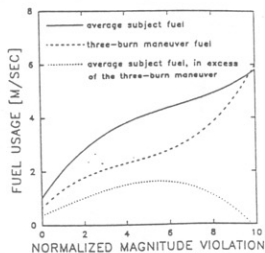


Fig. 4 Third-order regression curve of averaged-subject fuel use vs normalized magnitude violation score. The upward slope indicates that fuel use can be predicted from the violation score. The figure also shows the analytical regression curve for three-burn maneuver fuel use and the regression curve for the difference between the averaged-subject fuel use and 3-burn maneuver fuel use.

are drawn here brightly to indicate that departure and arrival velocity vectors have not yet been adjusted to fit the required constraints. Additional display attributes are the position of the target at intermediate waypoint time (12), additional vehicles like the orbiter (13), and a reference reticle in the center of the display (14).

Subject Background and Training

Seven subjects participated in the experiment. Three of them (ED, RE, RO) were airline pilots (DC-8, Boeing 737, P2, P5) of age 51–55 with 12,500–23,000 h of flight experience. One subject (DB) (age 54) was a retired navy pilot (A-4) with 5000 h of flight experience. The three remaining subjects (AJ, LK, SB) were nonpilot aerospace scientists aged 35–43. None of them, except two subjects (AJ, ED), were familiar with orbital operations and mechanics. Before beginning the experiment, the subjects carried out two 3-h training sessions usually completed in 1 day, in which they reviewed a training manual that interactively familiarized them with orbital mechanics and the various functions of the planning system. Finally, the manual guided them through a sample rendezvous planning mission in order to practice the display's controls and its operation.

Experimental Procedure

Data collection took about 8 hours and was generally spread across two days. Subjects were automatically presented through a UNIX C-shell script with the 90 rendezvous problems in four approximately equal groups of randomly ordered conditions. The following descriptive statistics were collected automatically by the IRIS computer: 1) planning time, 2) fuel use, 3) total number of way-points used, 4) operator activity such as number and type of operations and integral scores on the motion of waypoints in the planning process, and 5) a detailed account of constraint violations in the process, if any.

Results

Effect of Subject Instruction

Table 1 summarizes the average planning time and fuel use for 90 rendezvous planning missions, for each one of the subjects. The results show large variability between subjects. The subjects instructed to minimize fuel f on the account of planning time did not show significantly smaller fuel use [$F(1, 5) = 0.324$ $p < 0.594$] and those instructed to minimize the planning time t , did not have significantly shorter planning times, e.g., see RO and LK [$F(1, 5) = 2.033$ $p < 0.213$]. This indicates that the effect of subject instruction is highly masked by strong differences in basic planning strategy between the

subjects. Table 1 also shows the average subject performance for the t group, f group, and both groups.

Effect of Target Separation Parameters

Target separation parameters include the location of target separation above or below the V-bar, and the magnitude and direction of the separation velocity vector direction.

Anova analysis revealed significant effects of separation location and separation velocity vector direction on fuel use, ($F = 4.689$, $df = 9, 45$, $p < 0.001$) and ($F = 49.891$, $df = 7, 35$, $p < 0.001$), respectively. Since large individual differences in performance were found, it was preferable to describe these and other results by subject-to-subject regression analysis, presented here. Figures 2a-c show third-order regression curves for fuel use, planning time, and in-plane integrated waypoint displacement (in m) vs target separation velocity vector direction, where the angle is measured positive in the upward direction from the positive V-bar direction. The average subject curves for a particular group, i.e., t , f , or both, are the regressions for a set of 90 values, obtained by averaging each one of the 90 rendezvous scenarios across the subjects in each group. Multiple correlation values for each one of the regressions are listed in Table 2. All curves show clear maxima about the 180-deg angle, i.e., objects released in the backward or negative V-bar direction. For target separation in this direction, the spacecraft will move initially backward and downward with respect to the Space Station. An attempted two-burn maneuver to recover the target craft will result in the chaser passing right through the Space Station spatial constraint envelope [attribute (3) in Fig. 1]. In order to avoid the envelope, a third intermediate burn is needed. The intermediate waypoint can be placed such that the trajectory passes

either above or below the Space Station. Although the spatial constraints are satisfied, other constraints such as departure, arrival, plume impingement, and approach velocity constraints still have to be resolved. Figure 2a also shows analytical results of fuel use vs the separation velocity vector direction for two- and three-burn maneuvers. The location and time of arrival of the intermediate waypoint are chosen such that the trajectory just clears the envelope with minimum fuel cost. The minimum is empirically found to be unique. Although the fuel cost curve for the two-burn maneuver is almost flat, the curve for the three-burn maneuver shows a distinct maximum at about 180 deg. The difference between the curves can be attributed to the extra fuel cost involved in avoiding the Space Station envelope.

Figure 2a also shows that the average subject regression curves for the fuel usage, for the t , f , and both groups, are shifted upward with respect to the curve for the three-burn maneuver by a constant amount of 1 m/s. This indicates that the additional fuel needed to resolve the remaining constraint violations is independent of the target separation angle. The fuel use with the fuel optimizers is somewhat lower than that of the time optimizers.

A pronounced maximum at the 180-deg target separation velocity vector direction also appears in the regression curves for the planning time; see Fig. 2b. Surprisingly, the curve for the fuel optimizers is somewhat below that for the time optimizers, which indicates that instruction did not affect their absolute planning behavior. The strong increase in planning time for targets released in the backward direction can be attributed to both the time needed to position the third waypoint for clearing the structure, and the extra time needed to resolve other constraint violations resulting from this third

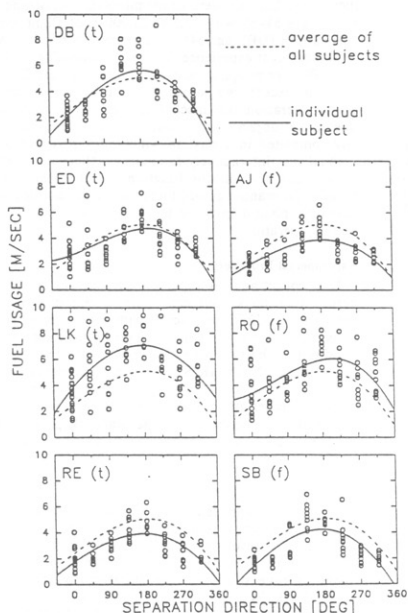


Fig. 5a Comparison of individual subject performance with performance, averaged over all subjects; third-order regression curves of fuel usage vs target separation velocity vector direction.

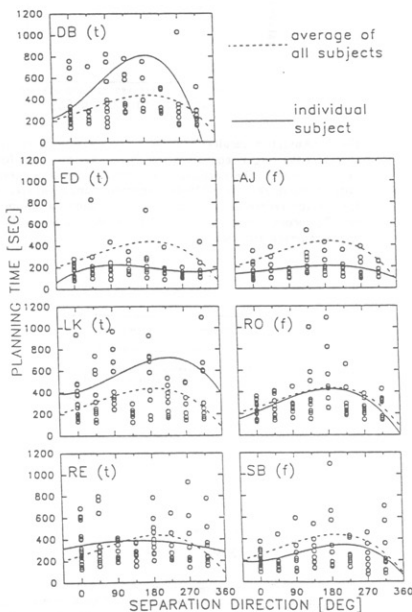


Fig. 5b Comparison of individual subject performance with performance, averaged over all subjects; third-order regression curves of planning time vs target separation velocity vector direction.

waypoint. A third waypoint placed considerably away from the unpowered two-burn trajectory will result in increased initial and terminal velocities and increased violations that, in turn, will demand longer planning times.

Similar maxima are found in the curves for the in-plane waypoint motion; see Fig. 2c. This indicates that for the targets separated in the backward direction, most of the additional planning time is devoted to the positioning of waypoints.

Measures for Predicting Fuel Expenditure and Planning Time

It is clear from the previous discussion that fuel expenditure and planning time will be closely related to the degree at which constraints are violated. A "violation score" has been composed as follows. Consider a three-burn maneuver with the third waypoint positioned such that the trajectory clears the spatial envelopes with minimum fuel. The resulting magnitude and angle violations at the departure gate and at arrival are treated separately. The amount of violation is normalized by dividing it by the allowable range and the normalized violations at departure and arrival are summed. Figure 3 shows the analytical results of the third-order regression curves of this violation score vs the separation angle. The normalized magnitude violation score shows a distinct maximum at the 225-deg angle and the normalized angular violation score a minimum at 180 deg. Added together, the effect of both scores is cancelled out, and the scores should therefore be treated separately. It is clear that the cost of avoiding the spatial envelope is primarily reflected in larger departure and arrival velocities and, therefore, a higher-magnitude violation. However, the effect of the third waypoint on the angular violation is highly

case-dependent. The normalized magnitude violation is therefore taken as the representative violation score.

Figure 4 shows how fuel use can be predicted from the violation score. The third-order regression curve of fuel expenditure vs violation score, averaged over all subjects, shows a distinct upward slope. This slope is due, to a large extent, to the characteristic of the analytical curve for the three-burn maneuver. The fuel use, in excess to the three-burn maneuver fuel, is used for resolving the remaining constraints; see the third regression curve in Fig. 4. Until four units of normalized violation score, the slope is upward and almost constant. Although the predictive value of the violation score is generally low, i.e., $R^2 = 0.14-0.40$, the predictive third-order regressions were statistically significant for all individual subjects. See Table 1.

No significant correlation was found between the violation score and planning time, which means that the violation score is not useful in predicting the planning time.

Subject Planning Characteristics

In Figs. 5a-c, fuel use, planning time, and in-orbital-plane waypoint activity of the individual subjects are compared. The dotted line indicates the average subject third-order regression curve, whereas the solid line is this curve for a particular subject. The regression multiple correlation values of the various curves are listed in Table 2. The strongest correlation is found for the fuel usage curves and the weakest for the planning time. Although the subjects show the same inverted u-shaped regression curves, large individual differences are noticed. Subjects DB and LK show, in particular, longer planning times and in-plane waypoint activity for the "difficult" separation directions. However, with LK the fuel use at these directions is especially high. This means that DB and LK did not effectively use the additional planning time for obtaining lower fuel use.

On the other hand, AJ and ED show rather "flat" regression curves for the planning time and in-plane waypoint activity, which indicates that they did not spend more time on the difficult maneuvers. Fuel use at these directions is found to be better than average.

In general, a strong similarity is found between the curves for planning time and in-plane waypoint activity. This means that additional planning time is used in moving around waypoints. This is true, in particular, for the strongly shaped u-curves of DB and LK, but also for the flat curves of RE. With RE the waypoint activity is especially low. Planning behavior is thus found to be strongly situation- and subject-dependent.

Discussion

The results of the present and previous experiments¹ have shown that after an initially short training period, operators can manually quickly plan complex orbital maneuvers, satisfying all operational constraints, when their planning tool is adapted to their capabilities. It is nonetheless also clear that properly programmed automatic systems could also plan these maneuvers. These results can help set performance criteria for these automatic systems since they should at least be capable of producing feasible plans in less than 2 min to beat a manually determined plan. Incorporation of all the mission constraints, however, can greatly complicate and lengthen an automatic search since these constraints may be arbitrarily placed in space and, in some cases, may be discrete. The proposed interactive technique might assist automatic optimizers by choosing good initial conditions. Certain constrained random search strategies could be adopted if more efficient analytical methods do not work well; see Soller et al.³

However, it is also clear that no matter how the maneuver is planned, any astronaut flying a mission would want to foresee what the system has planned for her and be able to visualize her trajectory, if for no other reason but to monitor its unfold-

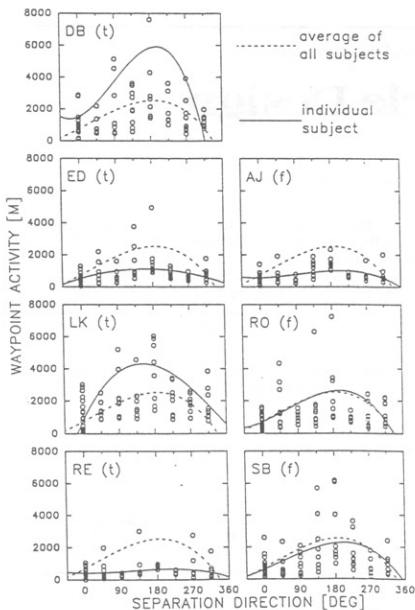


Fig. 5c Comparison of individual subject performance with performance, averaged over all subjects; third-order regression curves of in-plane waypoint activity versus target separation velocity vector direction.

ing as it is flown. Automatically generated trajectories will only be as good as the designer's hindsight in selecting optimization criteria and mission constraints. Unique mission features or failures may arise that require the custom-tailoring of a trajectory. Significantly, the mission-planning interface described in this paper also can serve as an interface to a mission "editor" that would allow an astronaut to visualize the automatically planned trajectories and edit them if necessary to suit her special requirements.

Absolute planning behavior is found to be strongly subject-dependent and hardly affected by subject instruction. On the other hand, fuel use and planning time are found to be affected by the target trajectory relative to spatial constraints. The higher multiple correlation values found for the fuel usage vs separation direction regression curves may be accounted for by the physical requirements associated with the mission, rather than human performance characteristics.

Violation scores on departure and arrival velocities would be useful in predicting the global amount of fuel use for a given mission. No measures have been found yet for predicting the necessary planning time.

The large variability in operator-planning behavior calls for standardizing planning strategies. At least three out of seven subjects were able to plan very fuel-efficient maneuvers within a reasonable planning time of about 300 s. Specific planning strategies of subjects with the best performance could be analyzed and used to compose a set of guidelines. These guidelines could be used either in an operator-training program or in expert systems to initialize or compose semiautomatic planning schemes.

The need for partial automatization in the planning procedure, such as the optimal positioning of a waypoint to clear a spatial envelope or satisfy departure or arrival constraints, is apparent when a uniform planning performance is desired over a wide range of situations and broad spectrum of operators. The automated system should be able to "suggest" a certain solution and quickly recompute a different solution when reviewed and changed by the operator. This will unburden the operator of planning time-consuming local optimizations. Efficient operator interaction with partially or fully automated planning schemes will require the development of local or global optimization schemes, for which the background computation time does not exceed several seconds.

References

- ¹Grunwald, A. J., and Ellis, S. R., "Interactive Orbital Proximity Operations Planning System," *Proceedings of the 1988 IEEE International Conference on Systems, Man, and Cybernetics* (Peking, China), IEEE CAT 88CH2556-9, 1988, pp. 1305-1312.
- ²Grunwald, A. J., and Ellis, S. R., "Interactive Orbital Proximity Operations Planning System," NASA TP 2839, Nov. 1988.
- ³Grunwald, A. J., and Ellis, S. R., "Design and Evaluation of a Visual Display Aid for Orbital Maneuvering," *Pictorial Communication in Virtual and Real Environments*, edited by S. R. Ellis, M. Kaiser and A. Grunwald, Taylor and Francis, London, 1991, pp. 207-231.
- ⁴Ellis, S. R., and Grunwald, A. J., "A New Illusion of Projected Three-Dimensional Space," NASA TM 100006, July 1987.
- ⁵Soller, J. A., Grunwald, A. J., and Ellis, S. R., "A Trajectory Planning Scheme for Spacecraft in the Space Station Environment," NASA TM 102866, Jan. 1991.

Recommended Reading from the AIAA Education Series



Space Vehicle Design

Michael D. Griffin and James R. French

"This is the most complete and comprehensive text on the subject of spacecraft design." — Marshall H. Kaplan, Applied Technological Institute

This authoritative text reflects the authors' long experience with the spacecraft design process. The text starts with an overall description of the basic mission considerations for spacecraft design, including space environment, astrodynamics, and atmospheric re-entry. The various subsystems are discussed, and in each case both the theoretical background and the current engineering practice are fully explained. Unique to this book is the use of numerous design examples to illustrate how mission requirements relate to spacecraft design and system engineering. Includes more than 170 references, 230 figures and tables, and 420 equations.

Table of Contents: (partial)

Mission Design - Environment - Astrodynamics - Propulsion - Atmospheric Entry - Attitude Determination and Control - Configuration and Structural Design - Thermal Control - Power - Telecommunications

1991, 465pps, illus., Hardback • ISBN 0-930403-90-8

AIAA Members \$47.95 • Nonmembers \$61.95 • Order #: 90-8 (830)

Place your order today! Call 1-800/682-AIAA



American Institute of Aeronautics and Astronautics
Publications Customer Service, 9 Jay Gould Ct., P.O. Box 753, Waldorf, MD 20604
Phone 301/645-5643, Dept. 415, FAX 301/843-0159

Sales Tax: CA residents, 8.25%; DC, 6%. For shipping and handling add \$4.75 for 1-4 books (call for rates for higher quantities). Orders under \$50.00 must be prepaid. Please allow 4 weeks for delivery. Prices are subject to change without notice. Returns will be accepted within 15 days.